

Facile Group IV Based C-H Bond Activation: Confirmation of Classic Benzyne Mechanism by DFT. Extension to Adamantyl Activation.

Motasem Suleiman,^{1,2} Fioralba Taullaj,¹ and Ulrich Fekl^{1,*}

Group IV organometallic complexes are promising systems for C-H bond activation. We are interested in the C-H bond activation of the CH₂ positions of the adamantyl group, since these positions are particularly hard to activate and to functionalize. As a potential platform for activation of that important alkyl group, we consider the alkyl bonded to the cyclopentadienyl in a substituted bis-cyclopentadienyl group IV metal diphenyl complex. The mechanism proposed in the classic paper reporting such activation using Zr(IV) (Erker and Mühlenbernd, 1987) involves an η^2 -benzyne complex intermediate. This current work reports a computational analysis of the problem through Density Functional Theory (DFT). We found that the two-step mechanism proposed for activation of C(Me)₂-Ph or *tert*-Bu groups using Zr(IV) is indeed confirmed by DFT and that it can be extended to Ti and Hf. We further found that the system can be successfully extended to the adamantyl group. The first step involves formation of the benzyne complex, which can also be described as a metallacyclopropene. In the second step, the cyclopentadienyl-bound alkyl is activated in the coordination sphere of the metal via proton transfer to the bound benzyne, which, if the metallacyclopropene description is chosen, resembles a σ -bond metathesis. The C-H bond activation of adamantyl through this approach is thermodynamically and kinetically feasible. Selective α -CH bond activation should be achievable with Ti (under thermodynamic control), and selective γ -CH bond activation with Zr (under kinetic or thermodynamic control).

¹ Department of Chemical and Physical Sciences
University of Toronto Mississauga, 3359 Mississauga Rd
Mississauga, Ontario, L5L 1C6, Canada

* indicates corresponding author. E-mail: ulrich.fekl@utoronto.ca

² Current address: Department of Mathematics
University of Toronto, Room 6290, 40 St. George Street,
Toronto, Ontario, M5S 2E4, Canada

Introduction

Adamantane is the simplest diamondoid (molecular nano-diamond).^[1,2,3] It is a hydrocarbon cage that contains 10 carbon atoms,^[1-3] in the form of 4 identical bridgehead positions (1-position; tertiary carbon center, methine position) and 6 identical bridge positions, (2-position; secondary carbon center, methylene position).^[1-3] The carbon atoms of adamantane are arranged in the same way as in the crystal lattice of diamond,^[1,2,4] which is the reason why it is called adamantane, after the Greek word for diamond.^[1,2]

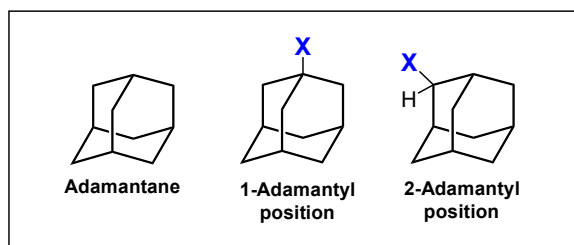


Figure 1. The structure of adamantane (left), the 1-adamantyl group bound to a substituent X (middle), and the 2-adamantyl group bound to a substituent X (right).

The structure of adamantane, along with the two isomeric adamantyl groups (1-adamantyl, 1-Ad; 2-adamantyl, 2-Ad), is shown in Figure 1. Adamantane is rigid and inert.^[1,3] These properties allow it to have numerous applications in different areas such as pharmacology, solid state NMR spectroscopy, and polymer chemistry.^[2,3,5,6] However, to achieve useful applications of adamantane, one must functionalize it selectively. The functionalization of adamantane is an important research topic.^[7,8,9] Most progress has been made related to functionalization of the 1-position.^[7-9,10,11,12] The only widespread functionalization of the 2-position is the production of adamantanone through oxidation of adamantane with $\text{H}_2\text{SO}_4/\text{SO}_3$.^[9,10,13,14] Our toolkit for elaborations on the adamantane

framework would be usefully enhanced, in particular for late-stage functionalization, if selective functionalization at the 2-position of adamantane could be accomplished using targeted organometallic C-H bond activation.^[15] C-H bond activation is the cleavage of a C-H bond by a metal complex; it may be followed by selective functionalization to form useful functional groups.^[16] Traditionally, late transition metals, which include noble metals like Pt, Pd, Rh and Ir are known for their ability to C-H activate,^[15,16,17,18,19,20,21] but C-H bond activation through early transition metals like Zr, Hf and Ti is also reported in literature.^[22] The mechanism for C-H bond activation is dictated by several factors, including; the type of the metal center, the oxidation state of the metal, and the ligands coordinating to the metal.^[16,18,20] Some of these mechanisms are shown in Figure 2.

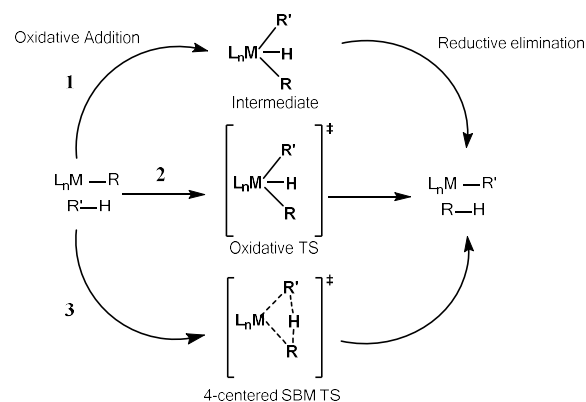


Figure 2. Selected mechanisms for C-H bond activation. Path 1 involves the formation of an intermediate through oxidative addition of $\text{R}'\text{-H}$, followed by reductive elimination of R-H . Path 2 involves the formation of oxidative transition state to achieve the C-H bond activation. Path 3 involves the formation of 4-centred σ -bond metathesis transition state for C-H bond activation.

Recently, a selective functionalization, namely a stereoselective fluorination, of the CH_2 position of a substituted (amino-substituted) adamantane was reported with a late transition metal (Pd).^[17] We would like to explore the

possibility of C-H bond activation through metal complexes with an early transition metal centre; Zr, Hf, and Ti. Due to the difficulty of forming direct M-C bonds between adamantane and an early metal, we sought to explore systems in which a tether can be used to bring the C-H bond of interest within proximity to the metal. Upon successful tethering, the ligand and the tethered substrate can be reacted with an early transition metal to form a metal complex. Further reactions on the metal complex can potentially achieve the desired C-H bond activation. Bent metallocene complexes are a good starting point for tethering the substrate of interest on a ligand coordinated to an early transition metal.^[23,24] Bent metallocene complexes containing the $\text{Cp}^{\text{R}}_2\text{M}$ substructure ($\text{Cp}^{\text{R}} = \text{cyclo-C}_5\text{H}_4\text{R}$, coordinated to early metal M in η^5 -fashion) have useful implementations in synthetic organic chemistry and they also have an active catalytic role in olefin polymerization chemistry.^[23,25,26,27]

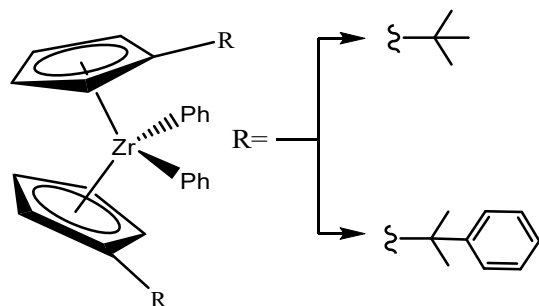


Figure 3. Structure synthesized by Erker et al.^[24]

In the course of work motivated by olefin polymerization, surprising and valuable discoveries of C-H activation were made. An example is the classic work of Erker and Mühlenbernd, in which $\text{Cp}^{\text{t-Bu}}_2\text{ZrPh}_2$ and $\text{Cp}^{\text{CMe}_2\text{Ph}}_2\text{ZrPh}_2$ were synthesized, shown in Figure 3.^[24] A thermolysis reaction of these compounds produced a cyclometallated complex through an intramolecular $\text{C}(sp^3)\text{-H}$ bond activation and $\text{C}(sp^2)\text{-H}$ bond activation for $\text{Cp}^{\text{t-Bu}}$ and $\text{Cp}^{\text{CMe}_2\text{Ph}}$,

respectively.^[24] It was hypothesized that the intramolecular C-H activation in the bent metallocene complexes proceeds via a reactive (η^2 -benzyne) zirconium complex intermediate through a hydrogen transfer.^[24]

This current contribution provides a computational (DFT) examination of the work reported by Erker et al., combined with useful extensions. We begin by thermodynamically studying the thermolysis reactions proposed by Erker et al. for structures provided in Figure 3 with three different metal centers: zirconium, where previous experimental data exist, but also extensions to titanium and hafnium. Next, we focus on assessing the suggested mechanistic pathway, which was proposed to go through a reactive η^2 -benzyne metal complex.^[24] Finally, we study the possibility of extending the work of Erker et al to C-H bond activation of adamantane tethered onto a Cp ligand (Cp^{Ad}) in a bent metallocene complex.

Methods

We performed geometry optimizations, without symmetry constraints, using DFT computations with the Gaussian 09 program^[28], using B3LYP^[28,29,30,31,32] as the functional. The basis set chosen was the Stuttgart-Dresden-Dortmund basis set employing effective core potentials (SDD).^[32,33,34,35,36] The initial structures were generated with GaussView and Chemcraft.^[28,37] The optimization of each structure was followed by a frequency computation in order to confirm the status as a local minimum.^[28,30,38] To locate the transition states, *Synchronous Transit-Guided Quasi-Newton* (STQN) methods were applied.^[28,30,39] The method was run through QST2 and QST3 commands.^[28,30] QST2 requires the optimized geometries of the reactant and the product, then the transition state is located via parabolic paths connecting the reactant and the product structures.^[28,30,39] QST3 is like QST2 but requires a geometrical guess of the

transition state structure for an enhanced parabolic path.^[28,30,39] A frequency computation was run directly after each transition state optimization, to confirm convergence of the computation to a true transition state, through the presence of exactly one imaginary frequency.^[28,30,39] Free energy diagrams were constructed using Hess's law from the output free energies, referencing the reactant state as zero.

Results and Discussion

Computational analysis of the experimental findings

Surprisingly, the 1987 work by Erker and Mühlenbernd^[24] has not been studied by DFT before. We obtained significant mechanistic findings that would have been difficult to obtain experimentally. Figure 4 and Figure 5 show the reaction schemes with the mechanism that was proposed by Erker et al., for the group(IV) metal mediated C-H activation of a *tert*-butyl (t-Bu), and a phenyl group, respectively. Figure 6 and 7 show free energy diagrams for the two different Zr mediated C-H activations which were reported by Erker et al. Table 1 summarizes the free energies for t-Bu activation, comparing the energetics for all three metals Zr, Hf and Ti, and Table 2 analogously for C(Me)₂Ph activation. In all cases, the reactions are thermodynamically favoured. As is clear from the summarized data in Tables 1-2, Ti and Zr provide the lowest energy barriers for the transition states, with barriers involving Hf being higher.

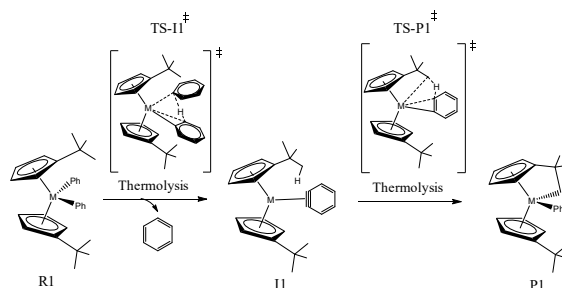


Figure 4. Reaction scheme for the C-H activation of Cp^{t-Bu} in Cp^{t-Bu}MPh₂ reported by Erker *et al.*^[24] R1 is the reactant, I1 is the intermediate, and P1 is the product. M represents either Zr, Hf or Ti. The experimental work is based on Zr.

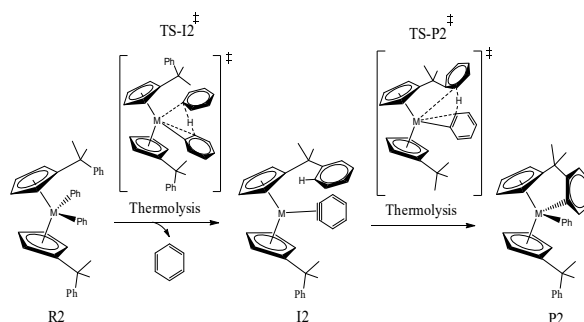


Figure 5. Reaction scheme for the C-H activation of Cp^{CMe₂Ph} in Cp^{CMe₂Ph}MPh₂. R2 is the reactant, I2 is the intermediate, and P2 is the product.^[24] M represents either Zr, Hf or Ti. The experimental work is based on Zr.

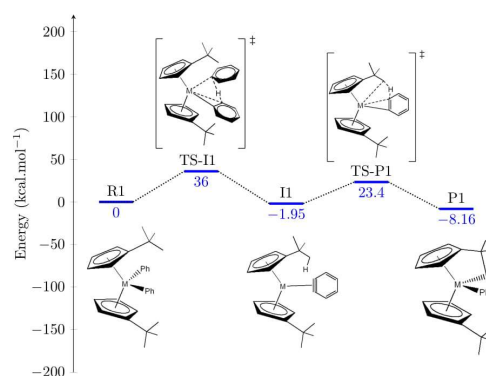


Figure 6. Free-energy profile for the formation of P₁ in the case of M=Zr. The thermolysis reaction of R₁ proceeds via the reactive I₁ intermediate.

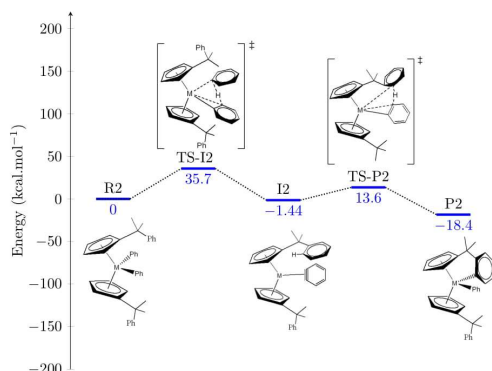


Figure 7. Free-energy profile for the formation of P₂ in the case of M=Zr. The thermolysis reaction of R₂ proceeds via the reactive I₂ intermediate.

Table 1. Summary of free energy values for M= Zr, Hf, Ti for the synthesis of P1. Energies are reported in (kcal/mol)

Metal	R1	TS-I1	I1	TS-P1	P1
Zr	0	36.0	-1.95	23.4	-8.16
Hf	0	40.2	0.94	27.9	-7.53
Ti	0	35	-15.2	16.5	-15.3

Table 2. Summary of free energy values for M= Zr, Hf, Ti for the synthesis of P2. Energies are reported in (kcal/mol)

Metal	R2	TS-I2	I2	TS-P2	P2
Zr	0	35.7	-1.44	13.6	-18.4
Hf	0	40.1	2.13	17.1	-17.9
Ti	0	34.8	-12.8	10.5	-21.6

For Ti, the activation barrier for the first step is about 35 kcal/mol, regardless of which exact substituted cyclopentadienyl is used (Tables 1 and 2). The second step (I1 to TS-P1 and I2 to TS-P2, data in Tables 1 and 2) has an activation barrier of 31.7 and 23.3 kcal/mol for the C-H activation of tBu and for phenyl, respectively. Zr is, for the two systems shown so far, very competitive with Ti for the C-H bond activation of Cp^R. The activation barrier for the first step is only marginally higher, at 36 kcal/mol compared to 35 kcal/mol for Ti. However, the second step has an activation barrier of only about 25.4 and 15.0 kcal/mol for the C-H activation of t-Bu and for phenyl, respectively. Given that the first step

is the rate-determining step for both metals, and given that the first barrier is very similar, almost identical reaction rates would be obtained for the Ti system and the Zr system. The Hf system is predicted to be much slower, with a (rate-determining) barrier that is the highest out of all three metals, at about 40 kcal/mol.

While no detailed kinetics have been published for the experimental system, it has been reported that R1 with M=Zr has achieved 80 % conversion (with 20 % unreacted R1) after 5 h at 80 °C in benzene.^[24] Assuming first-order behavior, this translates into a first-order rate constant of $8.9 \cdot 10^{-5} \text{ s}^{-1}$ at 80 °C, which further, assuming the validity of the Eyring-Polanyi equation, translates into an activation barrier ΔG^\ddagger of 27.2 kcal/mol at 80 °C, if the input parameters (5 h, 80 °C) are taken at face value. The computed barrier for the rate-determining step (here the first step) is 36.0 kcal/mol at 25 °C, which becomes (vibrational analysis performed for $T = 353.15 \text{ K}$) 36.2 kcal/mol at 80 °C. We note again that this is not a rigorous comparison, in part because we are trying to extract kinetics from one conversion percentage at one point in time at one temperature, where no error estimate for either the time or the temperature is available. However, since the computed barrier deviates by only about 9 kcal/mol from the crudely estimated experimental value, the computed barrier is certainly reasonable.

Most importantly, our work confirms the C-H activation mechanism postulated to proceed via the formation of an η^2 -benzyne reactive intermediate.^[24] We show this intermediate as containing π -bound benzyne in Figures 4-7 by convention. However, a resonance description as a metallacyclopentatriene deserves consideration (Figure 8).

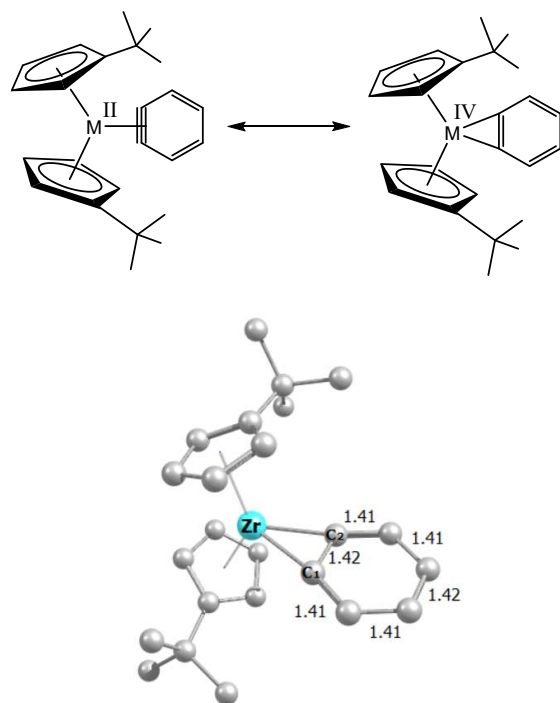


Figure 8. Resonance structures of I1 (top) along with the optimized intermediate structure of I1 (bottom, hydrogen atoms not shown).

The bond between the two metal-coordinated carbons would be expected to be particularly short, by virtue of its triple bond character, if the ligand were indeed a benzyne. Since the bond length in question is not shortened but similar to the other bond lengths in the C₆ ring, a bit longer, in fact, the metallacyclopentadiene description appears to be a good description. Bond distances are shown in Figure 8. This assignment is supported by a recent computational analysis using advanced methods for the analysis of ground state wave functions and densities (such as NBO, ELF, and AIM), which concluded for Cp₂Zr(C₆H₄) and the Hf analogue (but to a lesser degree for the Ti analogue), that in this resonance description the metallacyclic structure seems to have the larger weight.^[40]

This implies that the oxidation state of the metal centre remains the same throughout, with a value of +IV (d⁰). The mechanism of the C-H bond activation, broadly described as a proton

transfer, can thus be considered a σ -bond metathesis (SBM) mechanism, which typically requires that the centre metal should exist in its highest oxidation state.^[16,41] SBM is common for C-H bond activation with early transition metal complexes with the metal centre being in its highest oxidation state.^[16,41] Detailed structures of the transition states TS-I1 and TS-P1 are shown in Figure 9.

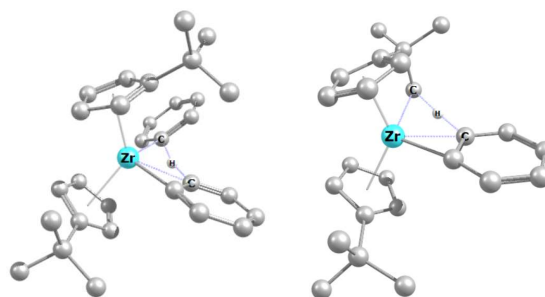


Figure 9. Optimized geometry for transition states TS-I1 (left) and TS-P1 (right), (hydrogen atoms on carbon are not shown).

Extending the work to adamantyl

The focus of this section is to validate the possibility of extending the existing work to C-H activation of adamantyls, in particular, selective activation of adamantyls at a methylene position.

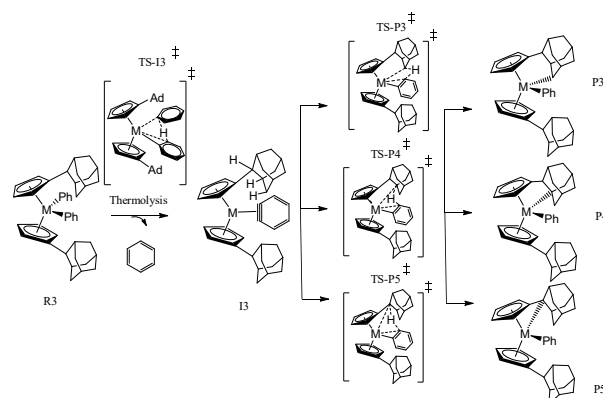


Figure 10. Proposed reaction scheme of the C-H activation of Cp₂-Ad in Cp₂-Ad₂MPh₂. R3 is the reactant, I3 is the intermediate, P3 is the γ -activated product, P4 is the β -

activated product and P5 is the α -activated product. M represents either Zr, Hf or Ti.

The proposed reaction scheme in Figure 10 was studied through DFT. One problem which arises from the reaction is the possibility of C-H activating a position other than the γ -position (P3) such as the α -position (P5) or β -position (P4). Gratifyingly, the results shown in Figure 11 and Table 3 illustrate that for Zr and Hf metals, the favoured product is the γ -CH₂-activated product. The formation of P3 is thermodynamically more stable by roughly 9 Kcal/mol when compared to P4. A slight difference in the energetics is observed when comparing P4 and P5 in which they differ by 2 Kcal/mol. However, for Ti (Table 3) the most stable thermodynamic product is P5, in which the α -position is activated. This is consistent with the work by Beckhaus et al., which has shown that titanium favours α -hydrogen abstraction much more than related zirconium and hafnium systems.^[42]

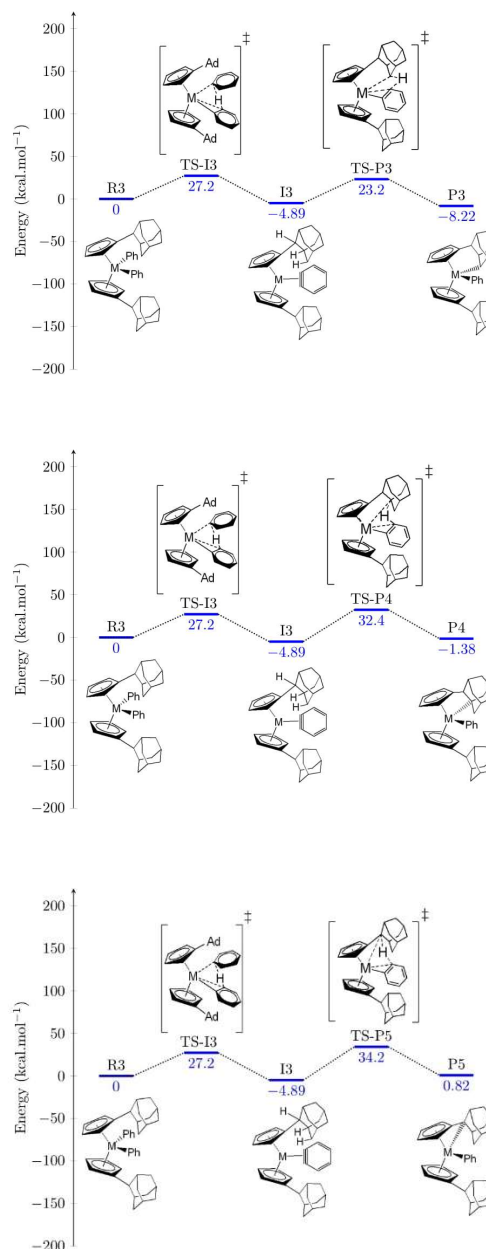


Figure 11. Free-energy profile for the synthesis of P3 (top), P4 (middle) and P5 (bottom). In the case of M=Zr. The thermolysis reaction of R3 proceeds via the reactive I3 intermediate. The free energies are reported relative to R3 and are obtained through DFT analysis.

Table 3a. Summary of free energy values for M= Zr, Hf, Ti for the synthesis of P3. Energies are reported in (kcal/mol)

Metal	R3	TS1-I3	I3	TS-P3	P3
Zr	0	27.2	-4.89	23.2	-8.22
Hf	0	31.5	1.07	28.0	-6.78
Ti	0	24.7	-15.1	17.8	-9.98

Table 3b. Summary of free energy values for M= Zr, Hf, Ti for the synthesis of P4. Energies are reported in (kcal/mol)

Metal	R3	TS1-I3	I3	TS-P4	P4
Zr	0	27.2	-4.89	32.4	-1.38
Hf	0	31.5	1.07	34.3	1.63
Ti	0	24.7	-15.1	25.9	-1.82

Table 3c. Summary of free energy values for M= Zr, Hf, Ti for the synthesis of P5. Energies are reported in (kcal/mol)

Metal	R3	TS1-I3	I3	TS-P5	P5
Zr	0	27.2	-4.89	34.2	0.816
Hf	0	31.5	1.07	38.5	3.64
Ti	0	24.7	-15.1	21.0	-12.9

From the standpoint of kinetics, the activation barriers for the first step were computed to be 27 kcal in the case of Zr, roughly 32 kcal/mol in the case of Hf and only 24 kcal for Ti as seen in Figure 11. The first step is achievable through a thermolysis reaction as shown in Erker's work. The second step is the crucial step in which the C-H activation of the γ -position has indeed the lowest activation barrier. Based on this, Zr is the best metal if γ -activation of a CH_2 group in the adamantyl is desired. This C-H activation can be accomplished as the second step, with an activation barrier of only 28.1 kcal/mol, much lower than the barriers for α - and β -activation (39.1 kcal/mol and 37.3 kcal/mol, respectively). The γ -activated product would be obtained not only due to kinetic control (lower barrier). If the system could equilibrate, for Zr, thermodynamic control would lead to the same product. If the α -activated product were desired, the computations suggest that Ti should be used, and the system should be equilibrated; under thermodynamic control the α -activated product would be obtained with titanium.

Conclusions

The C-H bond activation of adamantyl through a tethered approach was investigated with DFT methods, and the prior experimental work of Erker et al. on $\text{C}(\text{Me})_2\text{Ph}$ activation and $t\text{-Bu}$ activation was also studied with DFT. The C-H bond activation of aryl and alkyl groups tethered onto the Cp occurs via a reactive η^2 -benzynes complex intermediate, followed by the C-H activation step that is a σ -bond metathesis. The reactions were calculated to be thermodynamically and kinetically feasible. The experimentally known work was computationally extended to hafnium and titanium complexes, which showed similar reactivity. The C-H bond activation of adamantyl was shown to be feasible. The results suggest that Zr should be used, under either kinetic or thermodynamic control, to obtain the $\gamma\text{-CH}_2$ -activated product for adamantyl activation. Ti should be used, under thermodynamic control, if the α -activated adamantyl product is desired.

Funding Information

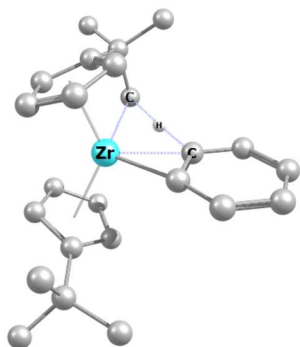
Funding by NSERC (Discovery Grant to UF) is gratefully acknowledged, as well as support by the University of Toronto Mississauga and the Department of Chemical and Physical Sciences, particularly in the form of access to a local computer cluster.

Keywords:

Adamantane. C-H Bond Activation. DFT. Sigma-Bond Metathesis. Metallocene

GRAPHICAL ABSTRACT

This DFT study investigates the C-H bond activation of tethered aryl and alkyl groups in an early transition metal sandwich complex. The mechanism involves a benzyne intermediate.

GRAPHICAL ABSTRACT FIGURE

References and Notes

- ¹ S. Landa, V. Macháček, *Collect. Czechoslov. Chem. Commun.* **1933**, 5, 1.
- ² R. C. Fort, P. R. Von Schleyer, *Chem. Rev.* **1964**, 64, 277.
- ³ H. Schwertfeger, A. A. Fokin, P. R. Schreiner, *Angew. Chem. Int. Ed.* **2008**, 47, 1022.
- ⁴ C. G. Windsor, D. H. Saunderson, J. N. Sherwood, D. Taylor, G. S. Pawley, *J. Phys. C Solid State Phys.* **1978**, 11, 1741.
- ⁵ C. R. Morcombe, K. W. Zilm, *J. Magn. Reson.* **2003**, 162, 476.
- ⁶ K. Spilovska, F. Zemek, J. Korabecny, E. Nepovimova, O. Soukup, M. Windisch, K. Kuca, *Curr. Med. Chem.* **2016**, 23, 3245.
- ⁷ B. A. Arndtsen, R. G. Bergman, T. A. Mobley, T. H. Peterson, *Acc. Chem. Res.* **1995**, 28, 154.
- ⁸ E. I. Bagrii, R. E. Safir, Y. A. Arinicheva, *Pet. Chem.* **2010**, 50, 1.
- ⁹ H. Bin Yang, A. Feceu, D. B. C. Martin, *ACS Catal.* **2019**, 9, 5708.
- ¹⁰ E. I. Bagrii, A. I. Nekhaev, A. L. Maksimov, *Pet. Chem.* **2017**, 57, 183.
- ¹¹ I. K. Moiseev, N. V. Makarova, M. N. Zemtsova, *Usp. Khim.* **1999**, 68, 1118.
- ¹² E. A. Shokova, V. V. Kovalev, *Russ. J. Org. Chem.* **2012**, 48, 1007.
- ¹³ M. M. Meyer, S. R. Kass, *J. Org. Chem.* **2010**, 75, 4274.
- ¹⁴ H. W. Geluk, J. L. M. A. Schlatmann, *Chem. Commun.* **1967**, 426.
- ¹⁵ R. H. Crabtree, *J. Organomet. Chem.* **2004**, 689, 4083.
- ¹⁶ R. H. Crabtree, *The Organometallic Chemistry of the Transition Metals*, John Wiley & sons, Inc., New Jersey, **2014**, pp 89-460.
- ¹⁷ Y. Q. Chen, S. Singh, Y. Wu, Z. Wang, W. Hao, P. Verma, J. X. Qiao, R. B. Sunoj, J. Q. Yu, *J. Am. Chem. Soc.* **2020**, 142, 9966.
- ¹⁸ J. A. Labinger, J. E. Bercaw, *Nature* **2002**, 417, 507.
- ¹⁹ X. Chen, K. M. Engle, D. H. Wang, Y. Jin-Quan, *Angew. Chem. Int. Ed.* **2009**, 48, 5094.
- ²⁰ K. Godula, D. Sames, *Science* **2006**, 312, 67.
- ²¹ U. Fekl, W. Kaminsky, K. I. Goldberg *J. Am. Chem. Soc.* **2003**, 125, 15286.
- ²² I. P. Rothwell, *Polyhedron*, **1985**, 4, 177.
- ²³ J. C. Green, *Chem. Soc. Rev.* **1998**, 27, 263.
- ²⁴ G. Erker, T. Mühlenbernd, *J. Organomet. Chem.* **1987**, 319, 201.
- ²⁵ E. P. Beaumier, A. J. Pearce, X. Y. See, I. A. Tonks, *Nat. Rev. Chem.* **2019**, 3, 15.
- ²⁶ U. Rosenthal, *Eur. J. Inorg. Chem.* **2019**, 2019, 895.
- ²⁷ M. Lamač, M. Horáček, J. Kubišta, J. Pinkas, *Inorganica Chim. Acta*, **2011**, 373, 291.
- ²⁸ M. J. Frisch, G. W. Trucks, H. B. Schlegel, G. E. Scuseria, M. A. Robb, J. R. Cheeseman, G. Scalmani, V. Barone, G. A. Petersson, H. Nakatsuji, X. Li, M. Caricato, A. V. Marenich, J. Bloino, B. G. Janesko, R. Gomperts, B. Mennucci, H. P. Hratchian, J. V. Ortiz, A. F. Izmaylov, J. L. Sonnenberg, D. Williams-Young, F. Ding, F. Lipparini, F. Egidi, J. Goings, B. Peng, A. Petrone, T. Henderson, D. Ranasinghe, V. G. Zakrzewski, J. Gao, N. Rega, G. Zheng, W. Liang, M. Hada, M. Ehara, K. Toyota, R. Fukuda, J. Hasegawa, M. Ishida, T. Nakajima, Y. Honda, O. Kitao, H. Nakai, T. Vreven, K. Throssell, J. A. Montgomery Jr., J. E. Peralta, F. Ogliaro, M. J. Bearpark, J. J. Heyd, E. N. Brothers, K. N. Kudin, V. N. Staroverov, T. A. Keith, R. Kobayashi, J. Normand, K. Raghavachari, A. P. Rendell, J. C. Burant, S. S. Iyengar, J. Tomasi, M. Cossi, J. M. Millam, M. Klene, C. Adamo, R. Cammi, J. W. Ochterski, R. L. Martin, K. Morokuma, O. Farkas, J. B. Foresman, D. J. Fox, Gaussian 16, Revision C.01, Gaussian, Inc., Wallingford, CT, **2016**.
- ²⁹ C. Lee, W. Yang, R. G. Parr, *Phys. Rev. B*, **1988**, 37, 785.
- ³⁰ J. B. Foresman, J. E. Frisch, *Exploring Chemistry with Electronic Structure Methods*, 3rd ed., Gaussian, Inc., Wallingford, CT, **2015**, p. 39.
- ³¹ A. D. Becke, *J. Chem. Phys.* **1993**, 98, 5648.
- ³² M. Dolg, U. Wedig, H. Stoll, H. Preuss, *J. Chem. Phys.* **1986**, 86, 866.
- ³³ D. A. H. Hanaor, M. H. N. Assadi, S. Li, A. Yu, C. C. Sorrell, *Comput. Mech.* **2012**, 50, 185.
- ³⁴ A. Bergner, M. Dolg, W. Küchle, H. Stoll, H. Preuß, *Mol. Phys.* **1993**, 80, 1431.
- ³⁵ M. Kaupp, P. V. R. Schleyer, H. Stoll, H. Preuss, *J. Chem. Phys.* **1991**, 94, 1360.
- ³⁶ M. Dolg, H. Stoll, H. Preuss, R. M. Pitzer, *J. Phys. Chem.* **1993**, 97, 5852.
- ³⁷ G. A. Zhurko Chemcraft, *Graphical Software for Visualization of Quantum Chemistry Computations*,

Ivanovo, Russia, **2005**.

<https://www.chemcraftprog.com>.

³⁸ S. F. Sousa, P. A. Fernandes, M. J. Ramos, *J. Phys. Chem. A*, **2007**, *111*, 10439.

³⁹ C. Peng, H. Bernhard Schlegel, *Isr. J. Chem.*, **1993**, *33*, 449.

⁴⁰ K. Miqueu, S. Labat, E. Daiann Sosa Carrizo, J. M. Sotiropoulos, *Eur. J. Inorg. Chem.* **2018**, *2018*, 2717.

⁴¹ R. Waterman, *Organometallics*, **2013**, *32*, 7249.

⁴² R. Beckhaus, C. Santamaría, *J. Organomet. Chem.* **2001**, *617*, 81.